Experimental and theoretical investigation of rate coefficients of the reaction S (P 3) + OCS in the temperature range of 298 – 985 K

Chih-Wei Lu, Yu-Jong Wu, Yuan-Pern Lee, R. S. Zhu, and M. C. Lin

Citation: The Journal of Chemical Physics **125**, 164329 (2006); doi: 10.1063/1.2357739
View online: http://dx.doi.org/10.1063/1.2357739
View Table of Contents: http://scitation.aip.org/content/aip/journal/jcp/125/16?ver=pdfcov
Published by the AIP Publishing

Experimental and theoretical investigation of rate coefficients of the reaction $S(^3P)+OCS$ in the temperature range of 298–985 K

Chih-Wei Lu and Yu-Jong Wu
Department of Chemistry, National Tsing Hua University, Hsinchu 30013, Taiwan

Yuan-Pern Lee[a)]
Department of Applied Chemistry, National Chiao Tung University, Hsinchu 30010, Taiwan; Institute of Molecular Science, National Chiao Tung University, Hsinchu 30010, Taiwan; and Institute of Atomic and Molecular Sciences, Academia Sinica, Taipei 10617, Taiwan

R. S. Zhu
Department of Chemistry, Emory University, Atlanta, Georgia 30322

M. C. Lin[b)]
Department of Applied Chemistry, National Chiao Tung University, Hsinchu 30010, Taiwan; Institute of Molecular Science, National Chiao Tung University, Hsinchu 30010, Taiwan; and Department of Chemistry, Emory University, Atlanta, Georgia 30322

(Received 14 April 2006; accepted 30 August 2006; published online 27 October 2006)

The reaction $S(^3P)+OCS$ in Ar was investigated over the pressure range of 50–710 Torr and the temperature range of 298–985 K with the laser photolysis technique. S atoms were generated by photolysis of OCS with light at 248 nm from a KrF excimer laser; their concentration was monitored via resonance fluorescence excited by atomic emission of S produced from microwave-discharged SO_2. At pressures less than 250 Torr, our measurements give $k(298\ \mathrm{K})=(2.7\pm0.5)\times10^{-15}$ cm^3 molecule^{-1} s^{-1}, in satisfactory agreement with a previous report by Klemm and Davis [J. Phys. Chem. **78**, 1137 (1974)]. New data determined for 407–985 K connect rate coefficients reported previously for $T\geqslant860$ and $T\leqslant478$ K and show a non-Arrhenius behavior. Combining our results with data reported at high temperatures, we derived an expression $k(T)=(6.1\pm0.3)\times10^{-18}\ T^{1.97\pm0.24}\exp[-(1560\pm170)/T]$ cm^3 molecule^{-1} s^{-1} for $298\leqslant T/\mathrm{K}\leqslant1680$. At 298 K and $P\geqslant500$ Torr, the reaction rate was enhanced. Theoretical calculations at the G2M(CC2) level, using geometries optimized with the B3LYP/6-311+G(3*df*) method, yield energies of transition states and products relative to those of the reactants. Rate coefficients predicted with multichannel Rice–Ramsperger–Kassel–Marcus (RRKM) calculations agree satisfactorily with experimental observations. According to our calculations, the singlet channel involving formation of SSCO followed by direct dissociation into $S_2(a\ ^1\Delta_g)+CO$ dominates below 2000 K; SSCO is formed via intersystem crossing from the triplet surface. At low temperature and under high pressure the stabilization of OCS_2, formed via isomerization of SSCO, becomes important; its formation and further reaction with S atoms partially account for the observed increase in the rate coefficient under such conditions. © *2006 American Institute of Physics*. [DOI: 10.1063/1.2357739]

I. INTRODUCTION

Carbonyl sulfide (OCS) commonly serves as a photolytic source of atomic sulfur in laboratories partly because the photofragment CO is practically inert. At large concentrations, the secondary reaction

$$S(^3P)+OCS\rightarrow \text{products} \qquad (1)$$

becomes important. Measurements of the rate coefficient k_1 at temperatures above 860 K using a shock tube and atomic absorption[1–4] yield results somewhat consistent with the activation energy, with E_a/R in the range of 3400–4560 K and the Arrhenius preexponential factor A in the range of $(39-100)\times10^{-12}$ cm^3 molecule^{-1} s^{-1}, except an earlier experiment that employed a shock tube with mass spectrometric product detection and yielded an erroneously small value of $k_1=1.0\times10^{-12}$ cm^3 molecule^{-1} s^{-1} at 2570 K.[5] In contrast, reported rate coefficients near 298 K using various detection methods differ significantly, in a range of $(0.2-54)\times10^{-15}$ cm^3 molecule^{-1} s^{-1}.[6–9] Table I summarizes rate coefficients reported for this reaction.

No experimental data exist for temperatures between 478 and 860 K. Extrapolation of the Arrhenius equation determined at high temperature yields k_1 at 298 K of 0.01–0.1 times the experimental values. A non-Arrhenius behavior for reaction (1) is thus indicated and warrants further characterization.

The reaction might proceed via various exothermic product channels:

a)Author to whom correspondence should be addressed. Electronic mail: yplee@mail.nctu.edu.tw
b)Author to whom correspondence should be addressed. Electronic mail: chemmcl@emory.edu

TABLE I. Summary of reported experimental rate coefficients using various methods.

Temperature (K)	Pressure (gas) (Torr)	k (~298 K) (10^{-15})[a]	A (10^{-12})[a]	E_a/R (K)	Method[b]	Reference
301	n.a.	⩾0.17			FP/GC and MS	Breckenridge and Taube (BT) (Ref. 8)
n.a.	n.a.	54				Gunning and Strausz (GS)(Ref. 9)
298–478	1294 (OCS/CO_2)	16	83	2525	FP/GC and MS	Jakubowski *et al.* (JALSGS) (Ref. 7)
233–445	20–200 (Ar)	3.48±0.39	1.52±0.20	1830±60	FP/RF	Klemm and Davis (KD) (Ref. 6)
860–1680	n.a.		50±8	3730±220	ST/ABS	Shiina *et al.* (SOYMM) (Ref. 1)
1140–1680	930–1740 (Ar)		39±12	3400±110	ST/ABS	Oya *et al.* (OSTM) (Ref. 2)
1200–1670	450–1500 (Ar)		99.7	4560	ST/ABS	Woiki *et al.* (WMR) (Ref. 4)
1750–2990	375–1035 (Ar)		6.6[c]		ST/ABS	Woiki and Roth (WR) (Ref. 3)
2570	365 (Ar)		1.0[d]		ST/MS	Hay and Berford (HB) (Ref. 5)
298–958	50–710 (Ar)	2.7±0.5	[e]	[e]	LP/RF	This work

[a]In units of cm^3 $molecule^{-1}$ s^{-1}.
[b]FP: flash photolysis; LP: laser photolysis; ST: shock tube; ABS: absorption; RF: resonance fluorescence; GC: gas chromatography; and MS: mass spectrometry.
[c]$k(1800-2200\ K)=6.6\times10^{-12}$ cm^3 $molecule^{-1}$ s^{-1}.
[d]$k(2570\ K)=1.0\times10^{-12}$ cm^3 $molecule^{-1}$ s^{-1}.
[e]$k(T)=(6.63\pm0.33)\times10^{-20}T^{2.57\pm0.19}\exp[-(1180\pm120)/T]$ cm^3 $molecule^{-1}$ s^{-1} for the temperature range of 233–1680 K.

$$S(^3P)+OCS(^1\Sigma^+)\rightarrow CO(X\ ^1\Sigma^+)+S_2(X\ ^3\Sigma_g^-), \quad (1a)$$

$$\Delta H_0=-28.8\ \text{kcal mol}^{-1},$$

$$\xrightarrow{M} OCS_2(^1A_1), \quad (1b)$$

$$\Delta H_0\cong-26\ \text{kcal mol}^{-1},$$

$$\xrightarrow{M} SSCO(^1A_1), \quad (1c)$$

$$\Delta H_0\cong-12\ \text{kcal mol}^{-1}.$$

The enthalpy of reaction for (1a) is derived based on the reported enthalpies of formation of 66.20 (S), −33.08 (OCS), −26.42 (CO), and 30.74 kcal mol^{-1} (S_2), respectively;[10] those of reactions (1b) and (1c) are estimated from quantum-chemical calculations, to be described hereafter. The presence of reaction (1b) was proposed by Basco and Pearson when they tried to explain their kinetic data for formation of S_2 following flash photolysis of CS_2 and OCS.[11] The other two possible reaction channels,

$$S(^3P)+OCS(^1\Sigma^+)\xrightarrow{M}SOCS(^1A'), \quad (1d)$$

$$\Delta H_0\cong21\ \text{kcal mol}^{-1},$$

$$S(^3P)+OCS(^1\Sigma^+)\rightarrow CS(^1\Sigma^+)+SO(^3\Sigma^-), \quad (1e)$$

$$\Delta H_0\cong35.1\ \text{kcal mol}^{-1},$$

are unimportant at low temperatures because they are quite endothermic. There has been no theoretical study of the kinetics of reaction (1).

We have earlier identified carbon disulfide S oxide (OSCS) and dithiiranone (OCS_2) using matrix isolation and infrared absorption techniques.[12] Irradiation of an Ar matrix sample containing O_3 and CS_2 with light at 248 nm from a KrF excimer laser yielded new absorption lines at 1402.1, 1056.2, and 622.3 cm^{-1}; these features were assigned to C═S stretching, O—S stretching, and S—C stretching modes, respectively, of OSCS. Annealing of this matrix to 30 K yielded new lines in a second set at 1824.7 and 617.8 cm^{-1}, assigned to C═O stretching and OCS bending modes of OCS_2, respectively. Calculations using density-functional theory (B3LYP/aug-cc-pVTZ) predicted four stable isomers: OCS_2, SSCO, OSCS, and SOCS, listed in order of increasing energy. According to calculations, OCS_2 has a C_{2v} symmetry and is the most stable; OSCS, SSCO, and SOCS are all planar. Calculated vibrational wave numbers, IR intensities, and ^{34}S- and ^{18}O-isotopic shifts for OSCS and OCS_2 fit satisfactorily with experimental results.

In this work, we have performed experiments on the reaction of S+OCS at pressures 50–710 Torr of Ar and extended rate measurements from 298 to 985 K to bridge the region $T\leqslant478$ K with a small activation energy and the region $T\geqslant860$ K in which the reported rate coefficients show an activation energy corresponding to $E_a/R=3400-4560$ K. The pressure dependence of rate coefficients at 298 K was investigated to confirm the existence of an adduct-formation channel under such conditions. We also performed detailed theoretical calculations to predict rate coefficients and to identify important channels in this reaction at various temperatures and pressures.

II. EXPERIMENTS

The experimental setup was described in detail previously;[13–15] only a brief description follows here. The reaction vessel is a six-way tubular quartz cross (with a diameter of 40 mm) with two sidearms of length ≅15 cm and with Brewster windows for laser photolysis. A temperature controller (Omega CN9000) regulated the temperature of the reactor through resistive heating. S atoms were produced on photolysis of OCS with radiation from a pulsed KrF excimer laser at 248 nm (0.5–19 mJ cm^{-2}, 0.5–3 Hz). Excess Ar gas was added to the system to ensure that $S(^1D)$ was quenched before reaction.[16] A microwave-discharge lamp with a flowing gas mixture of SO_2~0.10% in He produced emission in the transitions $S(^3S)$-$S(^3P_{2,1,0})$ at 180.73, 182.03, and

182.62 nm, respectively; the emission, collected with a lens (S1-UV, focal length $f=5$ cm, passing wavelength >170 nm), and excited S atoms in the reaction vessel for their detection.

The fluorescence was collected along an axis perpendicular to both photolysis laser and probe beams with a MgF_2 lens ($f=5$ cm) and detected with a solar-blind photomultiplier tube (EMR 541G-09). The signal was amplified with a low-noise amplifier (Stanford Research Systems, SR570) before being recorded with a digital oscilloscope (Tektronix, TDS-620B, 2.5 G sample s^{-1}, 500 MHz bandwidth). Temporal profiles for fluorescence of S were typically averaged over more than 500 laser pulses before being transferred to a computer for further processing.

OCS (99.98%, Matheson) was purified on distillation from trap to trap. A 20% mixture of OCS in Ar was prepared with standard gas-handling techniques. He (99.9995%) and Ar (99.9995%, both from AGA Specialty Gases) were used without further purification. The flow rates of He, Ar, and the OCS/Ar mixture were monitored with mass flow meters (Tylan FM360) that were calibrated with a wet testmeter or by the pressure increase in a calibrated volume before and after experiments.

Typical experimental conditions were as follows: total flow rate $F_T=10.7-13.3$ STP cm^3 s^{-1} (STP=1 atm and 273 K), reaction temperature $T=298-985$ K, total pressure $P=50-710$ Torr, $[OCS]=3.62\times10^{13}-1.05\times10^{17}$ molecule cm^{-3}, $[S]=(0.49-71.1)\times10^{11}$ molecule cm^{-3}, $[Ar]=(0.50-23.2)\times10^{18}$ molecule cm^{-3}, probed intervals of decay=20 μs–90 ms, and mean flow speed of the gaseous mixture $v=0.8-29.8$ cm s^{-1}.

III. COMPUTATIONAL METHODS

The geometries of the reactants, intermediates, transition states, and products of the title reaction were optimized at the B3LYP/6-311+G(3*df*) level of theory with Becke's three-parameter nonlocal exchange functional[17] and the nonlocal correlation functional of Lee *et al.*[18] Single point energies of all species were refined by the G2M(CC2) (Ref. 19) method using geometries and zero-point energies obtained at the B3LYP/6-311+G(3*df*) level. For the surface intersection points (MSX1 and MSX2), their geometries were located using the state-averaged complete active space self-consistent field (CASSCF) method.[20] Six electrons in six active spaces were used with 6-31+G(*d*) basis set. Because no symmetry was constrained in the geometry optimization, the default option in the GAUSSIAN program was used for the selection of the active space and electrons in the CASSCF calculation; the active space is defined assuming that the electrons come from the highest occupied orbitals in the initial guess determinant and that the remaining orbitals required for the active space come from the lowest virtuals of the initial guess. To be consistent with other species, vibrational wave numbers of these intersection points were approximately calculated at the B3LYP/6-311+G(3*df*,2*p*) level on the singlet surface. Imaginary wave numbers 293.8*i* and 420.1*i* cm^{-1} were obtained for MSX1 and MSX2, respectively, indicating that these points appear to have transition state characters. We confirm with GAUSSVIEW that MSX1 connects to the reactants and SSCO and MSX2 connects to the reactants and OCS_2. The total G2M(CC2) energy with zero-point energy (ZPE) correction is calculated as follows:

$$E[(\mathrm{G2M(CC2)}\ ] = E_{\mathrm{bas}} + \Delta E(+) + \Delta E(2df) + \Delta E(\mathrm{CC}) + \Delta' + \Delta E(\mathrm{HLC,CC2}) + \mathrm{ZPE}(3df,2p),$$

in which

$$E_{\mathrm{bas}} = E[\mathrm{PMP4/6\text{-}311G}(d,p)],$$

$$\Delta E(+) = E[\mathrm{PMP4/6\text{-}311+G}(d,p)] - E_{\mathrm{bas}},$$

$$\Delta E(2df) = E[\mathrm{PMP4/6\text{-}311G}(2df,p)] - E_{\mathrm{bas}},$$

$$\Delta E(\mathrm{CC}) = E[\mathrm{CCSD}(T)\mathrm{/6\text{-}311G}(d,p)] - E_{\mathrm{bas}},$$

$$\Delta' = E[\mathrm{UMP2/6\text{-}311+G}(3df,2p)] - E[\mathrm{UMP2/6\text{-}311+G}(2df,p)] - E[\mathrm{UMP2/6\text{-}311+G}(d,p)] - E[\mathrm{UMP2/6\text{-}311}(d,p)],$$

$$\Delta E(\mathrm{HLC,CC2}) = -5.78n_\beta - 0.19n_\alpha \quad \text{(in units of mhartree)},$$

in which n_α and n_β are the numbers of valence electrons, $n_\alpha \geqslant n_\beta$, and HLC indicates a higher level correction. For comparison, single point energies were also calculated at the CCSD(*T*)/6-311+G(3*df*) level based on the structures at the B3LYP/6-311+G(3*df*) level, expressed as CCSD(*T*)/6-311+G(3*df*)||B3LYP/6-311+G(3*df*). Calculations of the intrinsic reaction coordinate[21] (IRC) were performed to connect each transition state with designated reactants and products. All calculations were carried out with GAUSSIAN 03.[22]

Various statistical models for nonadiabatic reactions based on transition state theory (TST) have been developed and applied to a number of reactions.[23–34] All are based on the assumption that the minimum energy crossing point represents the transition state for the adiabatic reaction; the density of states of the transition state in the TST (or Rice–Ramsperger–Kassel–Marcus, RRKM) rate equation is then multiplied by "hopping probability" related to the spin-orbit coupling strength to correct the rate computed using the standard transition state theory for adiabatic processes. The results show that the one-dimensional treatment of the surface hopping probability often gives rate constants from about a factor of 2 (Ref. 34) to one to two orders of magnitude lower than experimental values.[29,33] In this work, the hopping probability via MSX1 and MSX2 was assumed to be unity. The standard adiabatic TST (or RRKM) theory as described in the following sections was employed to calculate rate constants.

The rate coefficients for various reaction channels were calculated with a multichannel RRKM [VARIFLEX] code (Ref. 35) which solves the master equation[36,37] involving multistep vibrational energy transfers for the excited intermediate SSCO or OCS_2. The Lennard-Jones (LJ) parameters

required for the RRKM calculations for the quenching of SSCO and OCS_2 were approximately taken the same as those of CS_2, with $\varepsilon/k=414.6$ K and $\sigma=4.575$ Å.[38] LJ parameters for Ar, $\varepsilon/k=114$ K and $\sigma=3.47$ Å, were also taken from Ref. 38. The exponential-down model with $\alpha=400$ cm^{-1} was employed for collisional deactivation. For the channels involved in two wells, a rigorous way of predicting their kinetics is to solve the time-dependent master equation (ME) which denotes a set of coupled integral differential equations of motion for populations of specific energy levels of the reactive intermediates:

$$\frac{\partial g_i(E,t)}{\partial t} = \omega \int_{E_{0i}}^{\infty} P_i(E,E')g_i(E',t)dE' - \omega g_i(E,t) - k_i(E)g_i(E) + r(E,t)$$

in which $g_i(E,t)$ is the population of energy level E in well i at time t, ω is the collisional frequencies, E_{0i} is the ground-state energy of well i, $P_i(E,E')$ is the transition probability for a molecule in well i with energy E' to go on collision to another state in the same well with energy E, $k_i(E)$ is the total rate constant of decay via all isomerization and decomposition channels open from well i at energy E, and $r(E,t)$ is the rate of formation for species i with energy E from the chemical activation and isomerization channels. The ME was solved in a matrix form with a method based on the Householder's tridiagonalization algorithm.[39] More details about the implementation of the time-dependent ME/RRKM analysis in CHEMRATE (Ref. 40) are available in a series of publications by Tsang and co-workers.[41–43] The accuracy of the method implemented in CHEMRATE was found to be adequate after examination through extensive comparisons with experimental and theoretical data for the reactions of phenyl with acetylene[44] and ethylene.[45] For the abstraction reaction channel not involving an intermediate, conventional TST theory was used to calculate the rate. Energies of the intermediates and transition states calculated at the G2M(CC2) level were used in the calculation of rate coefficients because the heats of reaction predicted by the method agree better with experimental values (*vide infra*).

IV. RESULTS AND DISCUSSION

A. Experimental rate coefficient below 250 Torr

All experiments were performed under pseudo-first-order conditions with [OCS]/[S] greater than 610. The initial concentration of S, $[S]_0$, was estimated from the absorption cross section (2.36×10^{-20} cm^2) of OCS and quantum yield $\Phi(S)=0.72\pm0.08$ at 248 nm,[46] and the fluence of the photolysis laser. The concentration of S atoms, $[S]_t$, follows an exponential decay. The apparent pseudo-first-order rate coefficient k^{Ia} is derived with the equation

$$\ln([S]_t/[S]_0) = -k^{Ia}t + at^2 + bt^3, \quad (2)$$

in which t is the reaction time and a and b are fitting parameters to account for secondary reactions.

To derive accurate rate coefficients, we employed a model comprising the following reactions:

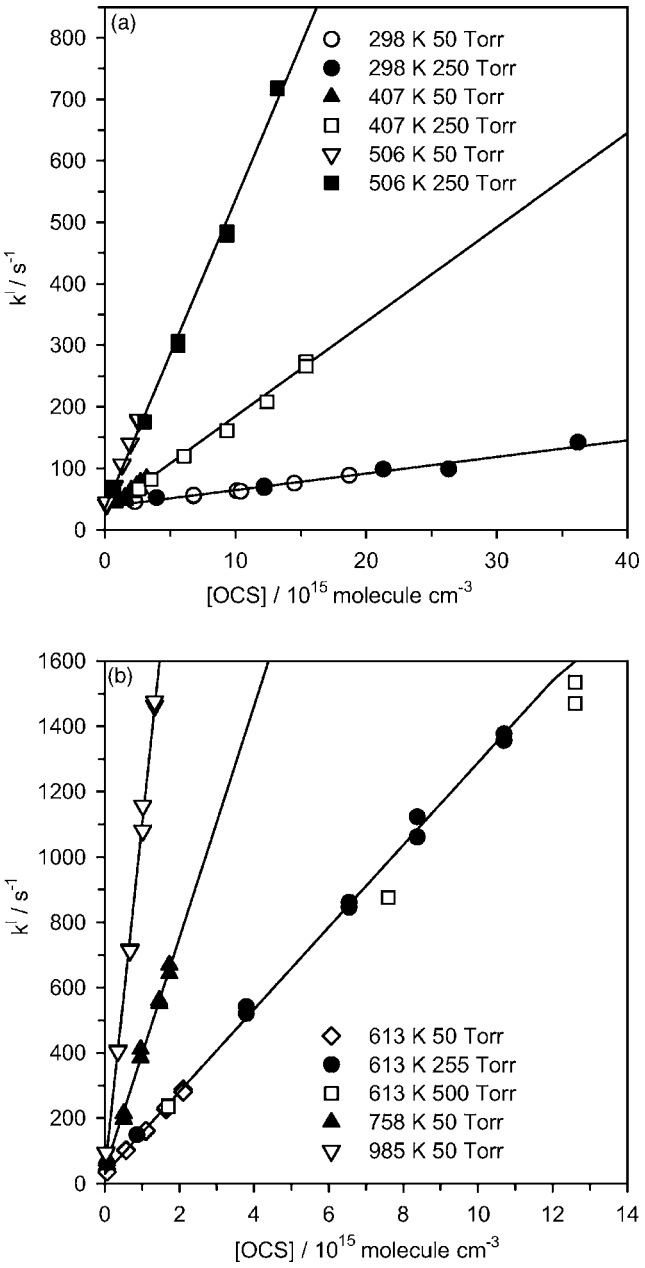

FIG. 1. Derived k^{I}_{1a} as a function of [OCS] at various temperatures. (a) 298 K, 50 Torr, symbol ○; 298 K, 250 Torr, symbol ●; 407 K, 50 Torr, symbol ▲; 407 K, 250 Torr, symbol □; 506 K, 50 Torr, symbol ▽; 250 Torr, symbol ■. (b) 613 K, 50 Torr, symbol ◇; 255 Torr, symbol ●; 758 K, 50 Torr, symbol ▲; 985 K, 50 Torr, symbol ▽. The data at 613 K and 500 Torr (symbol □) were not included in the fitting.

$$S(^3P) + OCS(^1\Sigma^+) \rightarrow CO(X\,^1\Sigma^+) + S_2(X\,^3\Sigma_g^-), \quad (1a)$$

$$\Delta H_0 = -28.8 \text{ kcal mol}^{-1},$$

$$\xrightarrow{M} OCS_2(^1A_1), \quad (1b)$$

$$\Delta H_0 \cong -26 \text{ kcal mol}^{-1},$$

$$S + OCS_2 \rightarrow S_2 + OCS, \quad (3)$$

TABLE II. Bimolecular rate coefficients k_1 at various temperatures.

T (K)	P (Torr)	[S] $(10^{11})^a$	[OCS] $(10^{14})^a$	[Ar] $(10^{17})^a$	k_1 (cm^3 $molecule^{-1}$ s^{-1})
298	51–250	9.0–42.8	5.45–362	16.4–79.9	$(2.7\pm0.5)\times10^{-15}$
407	50	10.5	7.68–32.0	11.9	$(1.5\pm0.2)\times10^{-14}$
506	50–250	1.87–7.65	1.39–132	9.5–49.3	$(5.0\pm0.8)\times10^{-14}$
613	50–255	0.81–9.75	0.60–107	7.9–40.2	$(1.3\pm0.2)\times10^{-13}$
758	50	0.84	0.63–17.3	6.4	$(3.6\pm0.5)\times10^{-13}$
985	51	0.49	0.36–13.3	5.0	$(1.0\pm0.2)\times10^{-12}$

[a]In units of molecule cm^{-3}.

$$S + S_2 \xrightarrow{M} S_3. \quad (4)$$

The calculated temperature dependence of the bimolecular rate coefficients k_{1b}^{II} and k_4^{III} at 50 Torr can be represented by

$$k_{1b}^{II}(T) = 9.08\times10^{7}T^{-7.59} \times\exp[-(3330/T)]\ cm^3\ molecule^{-1}\ s^{-1} \quad (5)$$

and

$$k_4^{III}(T) = 5.33\times10^{-20}T^{-4.12} \times\exp[-(625/T)]\ cm^6\ molecule^{-2}\ s^{-1}, \quad (6)$$

to be discussed later. The rate coefficient of reaction (3) is expected to be on the order of 10^{-10} cm^3 $molecule^{-1}$ s^{-1} because we found no barrier for this reaction.

We modeled observed temporal profiles of $[S]_t$ with reactions (1a), (1b), (3), and (4), with a commercial kinetic modeling program FACSIMILE;[47] rate coefficients listed in Eqs. (5) and (6) were unaltered and the pseudo-first-order rate coefficient of reaction (1a), k_{1a}^{I}, was varied to yield the best fit. According to our simulations, reactions (1b) and (3) are unimportant under our experimental conditions, and reaction (4) only has a small effect on the decay of S atoms. Values of k_{1a}^{I} thus derived are 78%–99% those of k^{Ia} derived with Eq. (2), supporting that reactions (1b) and (3) are unimportant under these conditions.

Values of k_{1a}^{I} determined with various concentrations of OCS at temperatures 298, 407, 506, 613, 758, and 985 K are plotted in Fig. 1; the slope of the line fitted with least squares yields the bimolecular rate coefficient k_{1a} at each temperature, as listed in Table II. Because reaction (1a) is dominant for reaction (1) under these conditions, we use values of k_{1a} to represent k_1. At 298 K, $k_1=(2.70\pm0.11)\times10^{-15}$ cm^3 $molecule^{-1}$ s^{-1}; unless otherwise noted, the uncertainty represents one standard error in fitting. In these experiments, rate coefficients remained the same while $[S]_0$ was varied by a factor of 12 and the total pressure was varied from 50 to 250 Torr. The combined systematic error (measurements of flow rates, pressure, and temperature) of our system is estimated to be ~9%, and the error in deriving k_{1a}^{I} and its dependence on [OCS] is ~15%. Hence, we estimate an error ~18% for k_1 and recommend a rate coefficient of $(2.7\pm0.5)\times10^{-15}$ cm^3 $molecule^{-1}$ s^{-1} at 298 K. The value of k_1 at 298 K determined in this work is within experimental uncertainties of the previous report of $k_1=(3.48\pm0.39)\times10^{-15}$ cm^3 $molecule^{-1}$ s^{-1} by Klemm and Davis,[6] but is smaller than two previous reports of rate coefficient determined relative to that of the reaction

$$S(^3P) + C_2H_4 \rightarrow \text{products}. \quad (7)$$

Jakubowski *et al.*[7] and Gunning and Strausz[9] reported ratios of $k_7/k_1=83$ and 25, respectively; the recommended rate coefficient of k_7 is 1.35×10^{-12} cm^3 $molecule^{-1}$ s^{-1},[48] which yields $k_1/10^{-15}$ cm^3 $molecule^{-1}$ $s^{-1}=16$ and 54, respectively. Even when the smallest reported value of $k_7=4.95\times10^{-13}$ cm^3 $molecule^{-1}$ s^{-1} (Ref. 49) is used, the derived values of $k_1/10^{-15}$ cm^3 $molecule^{-1}$ $s^{-1}=6$ and 20 are still much greater than ours at 298 K.

Rate coefficients k_1 determined at 298, 407, 506, 613, 758, and 985 K are listed in Table II; they are also compared with the previous data in Fig. 2 in which lines of various types are drawn for only the range of temperature investigated. Our data of k_1 increase from $(2.7\pm0.5)\times10^{-15}$ cm^3 $molecule^{-1}$ s^{-1} at 298 K to $(1.04\pm0.19)\times10^{-12}$ cm^3 $molecule^{-1}$ s^{-1} at 985 K, showing a distinct deviation from a linear Arrhenius form, but connecting satisfactorily data for $T>860$ K by Shiina *et al.*,[1] Oya *et al.*,[2] and Woiki *et al.*[3] and those for $T=233-445$ K by Klemm and Davis.[6]

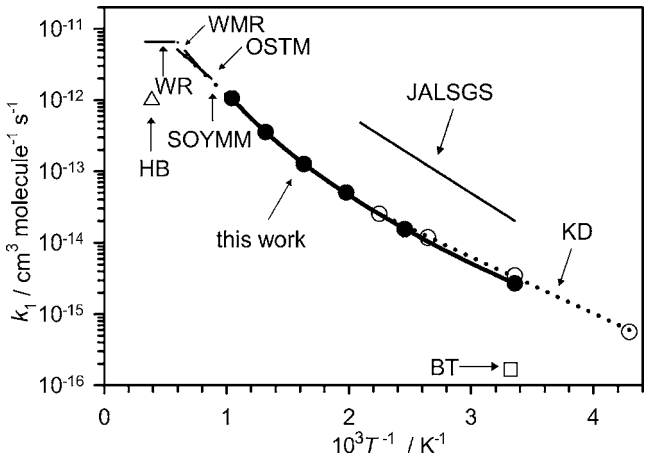

FIG. 2. Arrhenius plots of k_1 for the reaction $S+OCS\rightarrow S_2+CO$. Our data are shown as symbol ● with a fitted equation shown as a thick solid line. Those of Klemm and Davis (Ref. 6) are shown as symbol ○ with a fitted equation shown as a dotted line. Other previous results are shown as lines of various types drawn for the temperature range of study. A combination of first characters of each author's last name is used to indicate previous reports, as listed in Table I.

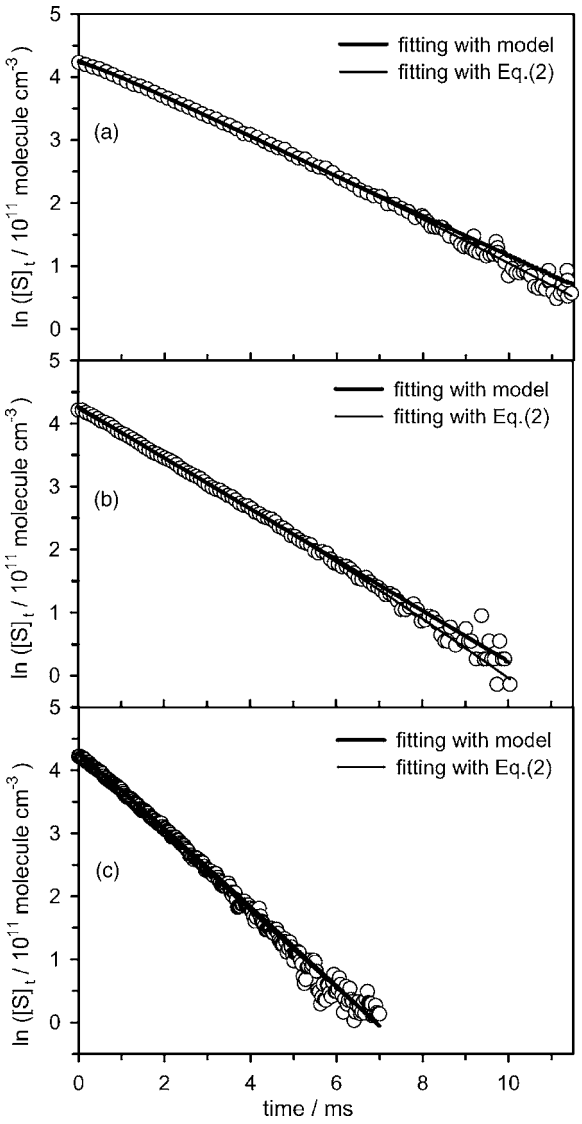

FIG. 3. Semilogarithmic plot of temporal profiles of $[S]_t$ observed after photolysis of a sample containing OCS and Ar. $T=298$ K, $P=710$ Torr, $[Ar]=2.3\times10^{19}$ molecule cm^{-3}, and $[OCS]/10^{16}$ molecule cm$^{-3}=0.66$ (a), 1.03 (b), and 5.31 (c). The solid line represents fitted results according to a model described in the text.

Fitting our results alone yields an expression for the rate coefficient in the range of $298 \leqslant T/\mathrm{K} \leqslant 985$:

$$k_1(T) = (2.86 \pm 0.14) \times 10^{-24} T^{3.97\pm0.12} \times \exp[-(580 \pm 60)/T] \text{ cm}^3 \text{ molecule}^{-1} \text{ s}^{-1}. \quad (8)$$

When combined with data for $T>860$ K reported by Oya *et al.*,[2] Woiki *et al.*,[3] and those for $T=233-445$ K by Klemm and Davis.,[6] we derive a general expression

$$k_1(T) = (6.63 \pm 0.33) \times 10^{-20} T^{2.57\pm0.19} \times \exp[-(1180 \pm 120)/T] \text{ cm}^3 \text{ molecule}^{-1} \text{ s}^{-1}, \quad (9)$$

for $233 \leqslant T/\mathrm{K} \leqslant 1680$. This equation reproduces reported rate coefficients within 25% except a few data points.

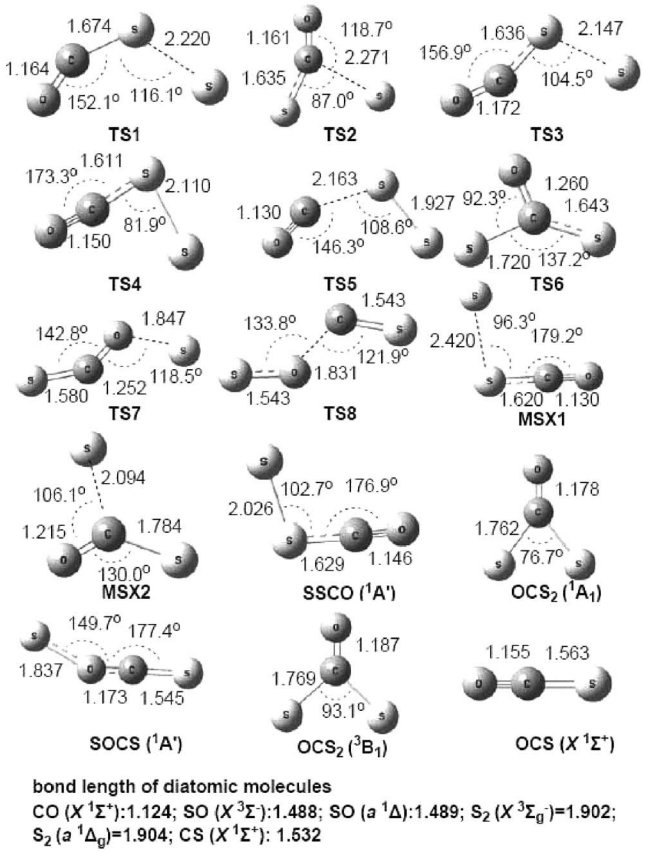

FIG. 4. Optimized geometries of transition states and intermediates of the S+OCS system at the B3LYP/6-311+G(3*df*) level, with bond lengths in angstrom and bond angles in degree.

B. Experimental rate coefficient at high pressures

We performed experiments also under high pressures. Although the decay deviates little from pseudo-first-order kinetics, a significant enhancement of an apparent pseudo-first-order rate coefficient k^{Ia}, derived according to Eq. (2), was observed for $P_T=500$ and 710 Torr at 298 K. Figure 3 shows a representative semilogarithmic plot of temporal profiles of [S] observed when a flowing gas mixture containing OCS and Ar at 710 Torr and 298 K was irradiated at 248 nm; the concentration of OCS was 0.66, 1.03, and 5.31×10^{16} molecule cm^{-3}. Values of $k_1/10^{-14}$ cm^3 molecule^{-1} s^{-1} were determined to be 5.0, 4.0, and 1.03 for $[OCS]/10^{16}$ molecule cm$^{-3}=0.66$, 1.03, and 5.31 under a total pressure of 710 Torr at 298 K. In contrast, values of k^{Ia} determined with various concentrations of OCS under a total pressure of 50, 255, and 510 Torr at 613 K are unaltered, as shown in Fig. 1. The observation indicates that, at low temperature and under high pressure, the channel involving formation of an adduct likely becomes important. We employed theoretical calculations to understand the mechanism, as discussed in the following section.

C. Potential-energy surfaces and reaction mechanism

Our calculations show that several triplet and singlet intermediates and transition states are involved in the reaction $S(^3P)+OCS\,(X\,^1\Sigma^+)$ to produce $S_2(X\,^3\Sigma_g^-)+CO(X\,^1\Sigma^+)$ and $S_2(a\,^1\Delta_g)+CO(X\,^1\Sigma^+)$. Optimized geometries of the inter-

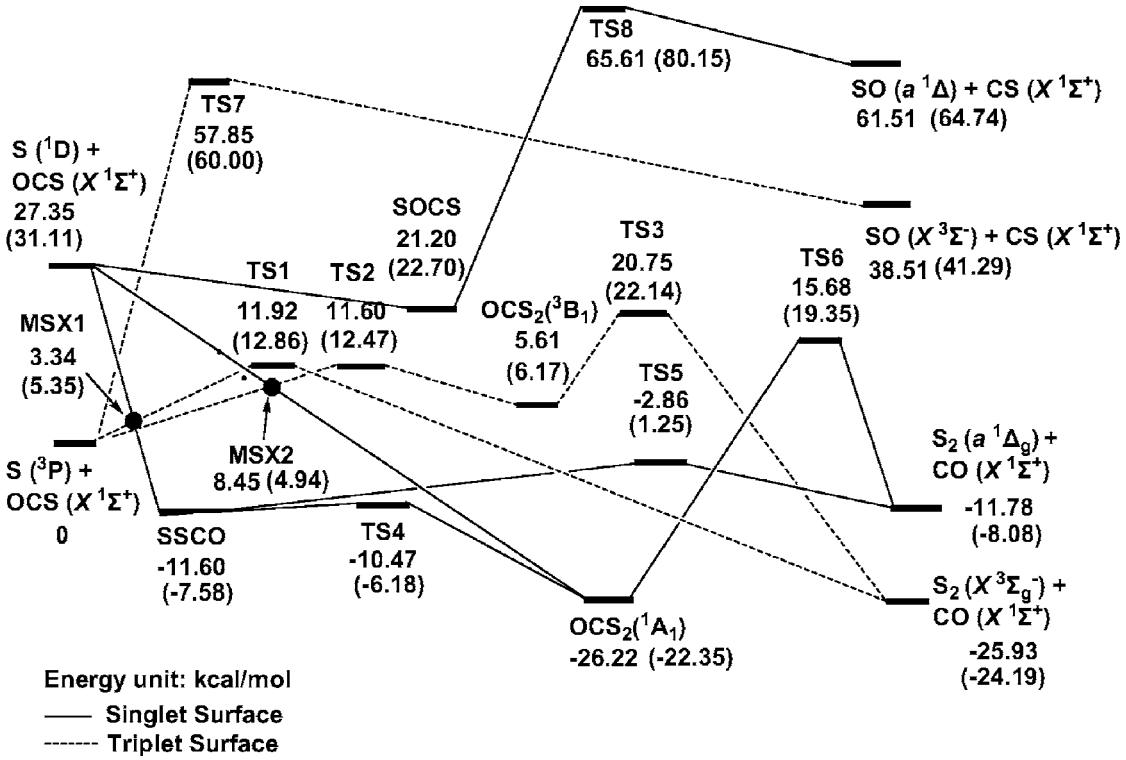

FIG. 5. Potential-energy diagrams for the S+OCS reaction based on energies calculated at the G2M(RCC2)||B3LYP/6-311+G(3*df*) level. Values in parentheses are calculated at the CCSD(*T*)/6-311+G(3*df*)||B3LYP/6-311+G(3*df*) level. Energies are listed in kcal mol^{-1}.

mediates and transition states involved in the reaction are shown in Fig. 4. The energy diagrams for singlet and triplet surfaces calculated with the G2M(CC2) and CCSD(*T*)/6-311+G(3*df*)||B3LYPY/6-311+G(3*df*) methods are presented in Fig. 5; values derived with the latter method are listed parenthetically. At the G2M(CC2) and CCSD(*T*)/6-311+G(3*df*)||B3LYPY/6-311+G(3*df*) levels, predicted enthalpies of reaction for S(^3P)+OCS($^1\Sigma^+$)$\rightarrow$CO($X\ ^1\Sigma^+$)+S$_2$($X\ ^3\Sigma_g^-$), −25.9 and −24.2 kcal mol^{-1} respectively, are 10% and 16% smaller than the value obtained from JANAF, −28.8 kcal mol^{-1}.[10] For formation of CO ($X\ ^1\Sigma^+$)+S$_2$($a\ ^1\Delta_g$), the predicted enthalpies of reaction are −11.8 and −8.1 kcal mol^{-1}, respectively, at the G2M(CC2) and the CCSD(*T*)/6-311+G(3*df*)||B3LYPY/6-311+G(3*df*) levels; experimental value from JANAF is −15.4 kcal mol^{-1}. For the production of SO ($^3\Sigma^-$)+CS($^1\Sigma^+$), the predicted enthalpies of reaction of 38.5 and 41.3 kcal mol^{-1} at the above levels may be compared with the JANAF value of 35.1 kcal mol^{-1}. The heat of formation of CS in JANAF (Ref. 10) has a large error of ~6 kcal mol^{-1}. The predicted enthalpies of reaction at the G3B3 level[50] for these three channels, −25.6, −9.8, and 37.0 kcal mol^{-1}, are in good agreement with values −25.9, −11.8, and 38.5 kcal mol^{-1} derived at the G2M(CC2) level. Comparing the enthalpies of reaction, we found that the values obtained at the G2M(CC2) level are closer to the experimental data. Accordingly, in the following text, values obtained at the G2M(CC2) level are cited. Predicted vibrational wave numbers and rotational parameters for the reactants, intermediates, transition states, and products are summarized in Table III. The experimental vibrational wave numbers are also listed in Table III for comparison;[12] predicted vibrational wave numbers deviate by less than 3% from experimental values.

Figure 5 shows that the triplet surface with the lowest energy proceeds via TS1 with a barrier of 11.9 kcal mol^{-1} to form S$_2$($X\ ^3\Sigma_g^-$)+CO($X\ ^1\Sigma^+$). The other triplet channel, proceeding via TS2 to form triplet OCS$_2$($^3B_1$) followed by decomposition to S$_2$($X\ ^3\Sigma_g^-$)+CO($X\ ^1\Sigma^+$) via TS3, has a much greater barrier. The reaction might also proceed via singlet surfaces by curve crossing via MSX1 and MSX2. Crossing via MSX1 at 3.3 kcal mol^{-1} produces SSCO ($^1A'$), which lies at −11 kcal mol^{-1} relative to the reactants and might subsequently decompose to S$_2$($a\ ^1\Delta_g$)+CO($X\ ^1\Sigma^+$) via TS5 (with a barrier 8.7 kcal mol^{-1}). SSCO ($^1A'$) may also isomerize to OCS$_2$($^1A_1$), lying at 26.2 kcal mol^{-1} below the reactants, via TS4 with a barrier of 1.1 kcal mol^{-1}. Crossing via MSX2 at 8.5 kcal mol^{-1} leads to formation of OCS$_2$($^1A_1$) directly. At low temperatures OCS$_2$ is unlikely to decompose to S$_2$($a\ ^1\Delta_g$)+CO($X\ ^1\Sigma^+$) because the energy of TS6 is about 15.7 kcal mol^{-1} above the reactants S(^3P)+OCS($X\ ^1\Sigma^+$). The predicted small barrier at TS4 for SSCO isomerization to OCS$_2$ is consistent with our earlier observation in low temperature matrices.

At low temperature and low pressure, crossing via MSX1 to form singlet SSCO, followed by decomposition of SSCO via TS5 to form S$_2$($a\ ^1\Delta_g$)+CO($X\ ^1\Sigma^+$), is the most important path. At higher temperatures, the direct abstraction channel via TS1 on the triplet surface becomes important; observed that activation energy of 7–9 kcal mol^{-1} at high temperatures is consistent with a predicted barrier of 11.9 kcal mol^{-1} for TS1.

Calculations based on transition state and RRKM theories were carried out with the VARIFLEX (Ref. 35) and CHEMRATE codes (Ref. 40) for the overall reaction,

$$S(^3P) + OCS \rightarrow \text{products} \tag{1}$$

via the following possible channels:

$$S + OCS \rightarrow TS1 \rightarrow S_2(X\,^3\Sigma_g^-) + CO(X\,^1\Sigma^+), \tag{1a-1}$$

$$S + OCS \xrightarrow{MSX1} SSCO(^1A') \rightarrow TS5 \rightarrow S_2(a\,^1\Delta_g) + CO(X\,^1\Sigma^+), \tag{1a-2}$$

$$S + OCS \xrightarrow{MSX2} OCS_2(^1A_1) \rightarrow TS6 \rightarrow S_2(a\,^1\Delta_g) + CO(X\,^1\Sigma^+), \tag{1a-3}$$

$$S + OCS \xrightarrow{MSX1} SSCO(^1A') \rightarrow TS4 \rightarrow OCS_2(^1A_1), \tag{1b-1}$$

$$S + OCS \xrightarrow{MSX2} OCS_2(^1A_1). \tag{1b-2}$$

The following scheme was used to couple all of the forward and reverse channels involved in the reactions:

$$\begin{array}{ccccc} & & S_2(a\,^1\Delta_g) + CO & & \\ & & \uparrow & & \\ S + OCS & \overset{k_1}{\rightleftharpoons} & SSCO^*(M) & \rightarrow & SSCO + M \\ & & \downarrow & & \\ S + OCS & \rightleftharpoons & OCS_2^*(M) & \rightarrow & OCS_2 + M \\ & & \downarrow & & \\ & & S_2(a\,^1\Delta_g) + CO & & \end{array}$$

For the constant prediction, the potential-energy surface (PES) obtained by both G2M(CC2) and CCSD(*T*)/6-311+G(3*df*)||B3LYP/6-311+G(3*df*) methods have been tested using the above reaction scheme; the result of the calculation based on the crossing energies at MSX1 obtained by the two methods (see Fig. 5), 3.3 and 5.3 kcal mol^{-1}, respectively, shows that the S disappearance rate is overpredicted by a factor of 2.4 at 300 K and 68% at 1000 K by the former method, and is underpredicted by 80% and 36% at the above two temperatures by the latter method. However, if the energy at MSX1 is adjusted up and down by 1.0 kcal mol^{-1} from those of G2M(CC2) and CCSD(*T*)/6-311+G(3*df*)||B3LYP/6-311+G(3*df*), respectively, to 4.3 kcal mol^{-1}, calculations based on both PES's lead to essentially the same values [see Fig. 6(b)], which also agree closely with experimental results over the temperature range studied. It should be mentioned that if the average frequencies calculated on the singlet and triplet surfaces at MSX1 and MXS2 were used, the predicted total rate constants increase by about 10% and 15% at 300 and 1000 K, respectively; the difference is well within the experimental scatters. The predicted individual and total rate constants based on the G2M(CC2) energetics and the frequencies on the singlet surface for MSX1 with the 4.3 kcal mol^{-1} barrier, as described above, can be expressed as

TABLE III. Vibrational wave numbers and rotational parameters for the reactants, intermediates, transition states, and products of the S+OCS reaction computed with the B3LYP/6-311+G(3*df*) method. Bold values in parentheses are experimental data taken from Ref. 12.

Species	I_a, I_b, I_c (GHz)	Vibrational wave numbers (cm^{-1})
SO ($a\,^1\Delta$)	21.4	1156.6
SO ($X\,^3\Sigma^-$)	21.4	1157.2
CS ($X\,^1\Sigma^+$)	24.7	1312.2
S_2 ($a\,^1\Delta_g$)	8.7	712.0
$^3S_2$ ($X\,^3\Sigma_g^-$)	8.7	716.1
CO ($X\,^1\Sigma^+$)	58.3	2217.1
OCS ($X\,^1\Sigma^+$)	6.1	531.3, 531.3, 879.4, 2115.5
OCS_2 ($^1A_1$)	6.6, 5.5, 3.0	363.0, 444.6, 523.9, 611.6 (**617.8**), 666.5, 1882.1 (**1824.7**)
OCS_2 ($^3B_1$)	6.4, 4.8, 2.7	288.2, 384.4, 510.9, 556.2, 611.0, 1801.8
SSCO ($^1A'$)	12.2, 2.9, 2.3	112.7, 402.3, 468.8, 502.9, 723.4, 2093.4
OSCS ($^1A'$)	30.2, 2.2, 2.0	134.7, 291.0, 488.0, 626.2 (**622.3**, **620.5**), 1062.4 (**1056.2**,**1052.7**), 1446.3 (**1402.1**, **1404.7**)
SOCS ($^1A'$)	123.3, 1.6, 1.6	63.7, 294.4, 436.4, 481.8, 904.9, 2036.0
TS1	11.9, 2.5, 2.1	336.1*i*, 134.0, 392.2, 435.5, 620.7, 1967.7
TS2	6.0, 4.0, 2.4	312.1*i*, 222.9, 397.1, 506.7, 755.7, 1998.3
TS3	12.1, 3.2, 2.5	417.5*i*, 274.0, 481.3, 588.8, 932.6, 1424.2
TS4	8.6, 3.8, 2.6	230.2*i*, 326.2, 468.5, 482.9, 796.3, 2106.7
TS5	11.2, 2.4, 2.0	239.2*i*, 64.4, 128.4, 281.9, 656.3, 2117.0
TS6	11.9, 3.2, 2.5	408.7*i*, 265.8, 499.8, 599.7, 964.1, 1426.8
TS7	17.4, 2.8, 2.4	487.7*i*, 293.4, 372.1, 615.5, 809.5, 1507.9
TS8	75.9, 1.5, 1.5	463.2*i*, 6.5, 186.9, 282.4, 938.9, 1242.5
MSX1	9.4, 2.5, 2.0	293.8*i*, 115.2, 454.2, 481.4, 587.9, 2078.8
MSX2	8.6, 2.7, 2.0	420.1*i*, 97.8, 359.8, 438.7, 449.6, 1528.8

$$k_{1a\text{-}1}(T) = 4.65 \times 10^{-14} T^{0.93} \times \exp[-(5980/T)]\ \text{cm}^3\ \text{molecule}^{-1}\ \text{s}^{-1}, \tag{10}$$

$$k_{1a\text{-}2}(T) = 1.27 \times 10^{-14} T^{0.96} \times \exp[-(2239/T)]\ \text{cm}^3\ \text{molecule}^{-1}\ \text{s}^{-1}, \tag{11}$$

$$k_{1a\text{-}3}(T) = 3.99 \times 10^{-21} T^{2.50} \times \exp[-(4769/T)]\ \text{cm}^3\ \text{molecule}^{-1}\ \text{s}^{-1}, \tag{12}$$

$$k_{1b\text{-}1}(T) = 7.65 \times 10^{9} T^{-8.22} \times \exp[-(4206/T)]\ \text{cm}^3\ \text{molecule}^{-1}\ \text{s}^{-1}, \tag{13}$$

$$k_{1b\text{-}2}(T) = 1.81 \times 10^{7} T^{-6.98} \times \exp[-(6046/T)]\ \text{cm}^3\ \text{molecule}^{-1}\ \text{s}^{-1}. \tag{14}$$

The predicted total rate coefficients ($k_{1a\text{-}1}+k_{1a\text{-}2}+k_{1a\text{-}3}+k_{1b\text{-}1}+k_{1b\text{-}2}$) are expressed as

$$k_1(T) = 1.43 \times 10^{-16} T^{1.58} \times \exp[-(1940/T)]\ \text{cm}^3\ \text{molecule}^{-1}\ \text{s}^{-1}, \tag{15}$$

in which $k_{1b\text{-}1}(T)$ and $k_{1b\text{-}2}(T)$ were calculated for $P=50$ Torr. The equations are in the temperature range of 298–2500 K. At 298 K, $k_{1b\text{-}1}=2.6\times10^{-17}$ and $k_{1b\text{-}2}=1.50\times10^{-19}$ cm^3 molecule^{-1} s^{-1}; for $T>1000$ K, $k_{1b\text{-}1}$

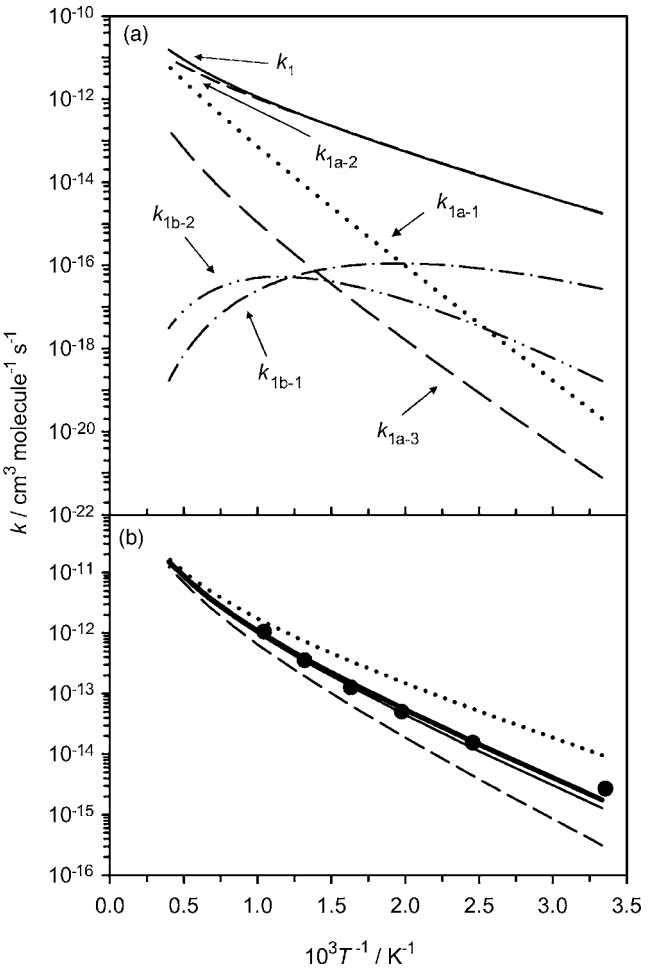

FIG. 6. (a) Theoretically predicted rate coefficients for the reaction S+OCS→products. Channel (1a-1): via TS1 on the triplet surface; channel (1a-2): via SSCO and TS5 on the singlet surface; channel (1a-3): via OCS_2 and TS6 on the singlet surface; channel (1b-1): via SSCO and TS4 to form OCS_2 on the singlet surface; channel (1b-2): via MSX2 to form OCS_2 on the singlet surface; solid line: total rate coefficient. (b) Comparison of experimental and calculated total rate coefficients. ●: experiment; dotted and dashed lines: calculated, using the PESs obtained at the G2M(CC2) and CCSD(T)/6-311+G(3df)‖B3LYP/6-311+G(3df) levels without any adjustment; thick and thin solid lines: calculated, based on the PESs predicted by the two methods using the same 4.3 kcal mol^{-1} energy at MSX1, respectively.

is less than 2.5×10^{-17} cm^3 molecule^{-1} s^{-1}. For the channels via MSX1 and MSX2, the calculations assume a unity probability for crossing from the triplet surface to the singlet surface. In view of the fact that the system involves two sulfur atoms, this assumption is expected to be valid.

Channel (1a-2) is clearly the dominating path at temperatures below 1500 K, whereas channel (1a-1) becomes non-negligible at temperatures above 1500 K, resulting in a more rapid increase of the rate coefficient at high temperatures. Formation rate of S_2 ($a\ ^1\Delta_g$)+CO ($X\ ^1\Sigma^+$) via the intermediate OCS_2 ($^1A_1$) is negligible because of the higher barrier of TS6. Rate coefficients for each channel and the total rate coefficient, Eqs. (10)–(15), are plotted in Fig. 6(a); the total rate constants predicted using the PES obtained by the above two methods and those with 1.0 kcal mol^{-1} adjustment for MSX1 are plotted in Fig. 6(b), the experimental results are also plotted for comparison. The total rate coefficient with MSX1=4.3 kcal mol^{-1} agrees satisfactorily with experimental results in this work, and also with those at high temperatures reported by Shiina *et al.*,[1] Oya *et al.*,[2] and Woiki *et al.*[3]

D. Kinetic modeling for reactions under high pressure at low temperature

According to calculations, the stabilization of SSCO that was formed via MSX1 is negligible because the barrier for further reaction is small. Stabilization of OCS_2 via channels (1b-1) and (1b-2) is negligibly small at low pressure, but becomes important at higher pressures. The pressure dependences of k_{1b-1} and k_{1b-2} at 298 K in the pressure range of 0.0263–1.316 atm were calculated to be

$$k_{1b-1}[M] = 1.76\times10^{-16}(P/P^0)^{0.56} \times\exp[-(0.01287P^0/P)]\ \text{cm}^3\ \text{molecule}^{-1}\ \text{s}^{-1} \quad (16)$$

and

$$k_{1b-2}[M] = 9.25\times10^{-19}(P/P^0)^{0.56} \times\exp[-(0.0129P^0/P)]\ \text{cm}^3\ \text{molecule}^{-1}\ \text{s}^{-1}, \quad (17)$$

in which P^0 represent the pressure, 1 atm, of the standard state. At 298 K, k_{1b-1} $[M]$ is 3.15×10^{-17} cm^3 molecule^{-1} s^{-1} at 50 Torr, whereas k_{1b-1} $[M]$ becomes 1.65×10^{-16} cm^3 molecule^{-1} s^{-1} at 700 Torr. The stabilization of OCS_2 via channel (1b-2) is negligible, with k_{1b-2} $[M]=1.66\times10^{-19}$ cm^3 molecule^{-1} s^{-1} at 50 Torr and k_{1b-2} $[M]=8.71\times10^{-19}$ cm^3 molecule^{-1} s^{-1} at 700 Torr.

We modeled observed temporal profiles of $[S]_t$ with the mechanism described in Sec. IV A [Eqs. (1a), (1b), (3), and (4)] using the modeling program FACSIMILE;[47] the rate coefficient k_{1a} obtained under 250 Torr remains unaltered. The values of $k_{1b-1}=1.65\times10^{-16}$ cm^3 molecule^{-1} s^{-1} for P =700 Torr and T=298 K were used for k_{1b}. The pressure dependences of k_4 at 298 K in the pressure range of 0.0263–2.63 atm was calculated to be

$$k_4[M] = 4.11\times10^{-12}(P/P^0)^{0.76} \times\exp[-(0.00995P^0/P)]\ \text{cm}^3\ \text{molecule}^{-1}\ \text{s}^{-1}, \quad (18)$$

with k_4 $[M]=3.83\times10^{-12}$ cm^3 molecule^{-1} s^{-1} at 700 Torr and 298 K. Simulated decay curves are shown as solid lines in Fig. 3; they are in satisfactory agreement with experimental observation. The enhancement in rate coefficient results partially from the increase in k_{1b-1} (~40% of k_{1a}) and partially from secondary reactions of S with OCS_2 and S_2; the latter was also enhanced at high pressure.

V. CONCLUSION

Rate coefficients for the reaction of S with OCS in the temperature range of 298–985 K have been determined. Our result at 298 K, $k_1=(2.7\pm0.5)\times10^{-15}$ cm^3 molecule^{-1} s^{-1}, is consistent with a previous measurement by Klemm and Davis.[6] Our new data in the range of 407–985 K fill the gap

between reported rate coefficients for $T \leqslant 478$ K and $T \geqslant 860$ K. From the combined available data, rate coefficients fit well with the equation $k_1 \quad (T) = (6.63 \pm 0.33) \times 10^{-20} T^{2.57 \pm 0.19} \exp[-(1180 \pm 120)/T]$ cm^3 molecule^{-1} s^{-1} for the temperature range of 233–1680 K; listed uncertainties represent one standard error in fitting. Theoretical calculations based on a PES computed at the G2M(CC2)//B3LYP/6-311+G(3*df*) level indicate that, at low temperature, the reaction proceeds via curve crossing to the singlet surface to form SSCO, followed by decomposition to S_2 ($a\ ^1\Delta_g$)+CO($X\ ^1\Sigma^+$); at high temperatures, a direct abstraction reaction to form S_2 ($X\ ^3\Sigma_g^-$)+CO($X\ ^1\Sigma^+$) on the triplet surface becomes competitive. Predicted total rate coefficients agree with experiments throughout the temperature range under investigation. According to calculations, the stabilization of OCS_2 is enhanced under high pressures and at low temperature. Secondary reactions of S with OCS_2 and S_2 result in an enhanced decay of [S], as was observed in our experiments.

ACKNOWLEDGMENTS

One of the authors (Y.P.L.) thanks the National Science Council of Taiwan (Grant No. NSC95-2119-M-009-032) and National Chiao Tung University for support. Another author (R.S.Z.) thanks the Office of Naval Research, US Navy (Contract no. N00014-89-J1949) for support. Also one of the authors (M.C.L.) acknowledges support from the Taiwan Semiconductor Manufacturing Company for the TSMC distinguished professorship and the National Science Council of Taiwan for a distinguished visiting professorship.

[1] H. Shiina, M. Oya, K. Yamashita, A. Miyoshi, and H. Matsui, J. Phys. Chem. **100**, 2136 (1996).
[2] M. Oya, H. Shiina, K. Tsuchiya, and H. Matsui, Bull. Chem. Soc. Jpn. **67**, 2311 (1994).
[3] D. Woiki and P. Roth, Ber. Bunsenges. Phys. Chem. **10**, 1347 (1992).
[4] D. Woiki, M. W. Markus, and P. Roth, J. Phys. Chem. **97**, 9682 (1993).
[5] A. J. Hay and R. L. Belford, J. Chem. Phys. **47**, 3944 (1967).
[6] R. B. Klemm and D. D. Davis, J. Phys. Chem. **78**, 1137 (1974).
[7] E. Jakubowski, M. G. Ahmed, E. M. Lown, H. S. Sandhu, R. K. Gosavi, and O. P. Strausz, J. Am. Chem. Soc. **94**, 4094 (1972).
[8] W. H. Breckenridge and H. Taube, J. Chem. Phys. **53**, 1750 (1970).
[9] H. E. Gunning and O. P. Strausz, Adv. Photochem. **4**, 143 (1966).
[10] M. W. Chase, Jr., J. Phys. Chem. Ref. Data Monogr. **9**, 1 (1998).
[11] N. Basco and A. E. Pearson, Trans. Faraday Soc. **63**, 2684 (1967).
[12] W.-J. Lo, H.-F. Chen, P.-H. Chou, and Y.-P. Lee, J. Chem. Phys. **121**, 12371 (2004).
[13] C.-W. Lu, Y.-J. Wu, Y.-P. Lee, R. S. Zhu, and M. C. Lin, J. Chem. Phys. **121**, 8271 (2004).
[14] E. W.-G. Diau and Y.-P. Lee, J. Chem. Phys. **96**, 377 (1992).
[15] L.-H. Lai, Y.-C. Hsu, and Y.-P. Lee, J. Chem. Phys. **97**, 3092 (1992).
[16] G. Blake and L. E. Jusinski, J. Chem. Phys. **82**, 789 (1985).
[17] A. D. Becke, J. Chem. Phys. **98**, 5648 (1993); **96**, 2155 (1992); **97**, 9173 (1992).
[18] C. Lee, W. Yang, and R. G. Parr, Phys. Rev. B **37**, 785 (1988).
[19] A. M. Mebel, K. Morokuma, and M. C. Lin, J. Chem. Phys. **103**, 7414 (1995).
[20] N. Yamamoto, T. Vreven, M. A. Robb, M. J. Frisch, and H. B. Schlegel, Chem. Phys. Lett. **250**, 373 (1996).
[21] C. Gonzalez and H. B. Schlegel, J. Phys. Chem. **90**, 2154 (1989).
[22] M. J. Frisch, G. W. Trucks, H. B. Schlegel *et al.*, GAUSSIAN 03, Revision A.1, Gaussian Inc., Pittsburgh, PA, 2003.
[23] G. E. Zahr, R. K. Preston, and W. H. Miller, J. Chem. Phys. **62**, 1127 (1975).
[24] E. J. Heller and R. C. Brown, J. Chem. Phys. **79**, 3336 (1983).
[25] A. J. Marks and D. L. Thompson, J. Chem. Phys. **96**, 1911 (1992).
[26] S. Hammes-Schiffer and J. C. Tully, J. Chem. Phys. **103**, 8528 (1995).
[27] M. S. Topaler and D. G. Truhlar, J. Chem. Phys. **107**, 392 (1997).
[28] Q. Cui, K. Morokuma, J. M. Bowman, and S. J. Klippenstein, J. Chem. Phys. **110**, 9469 (1999).
[29] J. C. Lorquet and B. Leyh-Nihant, J. Phys. Chem. **92**, 4778 (1988).
[30] M. Aschi and F. Grandinetti, J. Chem. Phys. **111**, 6759 (1999).
[31] J. N. Harvey, S. Grimme, M. Woeller, S. D. Peyerimhoff, D. Danovich, and S. Shaik, Chem. Phys. Lett. **322**, 358 (2000).
[32] P. R. P. De Moraes, H. V. Linnert, M. Aschi, and J. M. Riveros, J. Am. Chem. Soc. **122**, 10133 (2000).
[33] J. N. Harvey and M. Aschi, Faraday Discuss. **124**, 129 (2003).
[34] A. M. Mebel, M. Hayashi, V. V. Kislov, and S. H. Lin, J. Phys. Chem. A **108**, 7983 (2004).
[35] S. J. Klippenstein, A. F. Wagner, R. C. Dunbar, D. M. Wardlaw, and S. H. Robertson, VARIFLEX, Version 1.00, 1999.
[36] R. G. Gilbert and S. C. Smith, *Theory of Unimolecular and Recombination Reactions* (Blackwell Scientific, Carlton, 1990).
[37] K. A. Holbrook, K. J. Pilling, and S. H. Robertson, *Unimolecular Reactions* (Wiley, Chichester, 1996).
[38] F. M. Mourits and F. H. A. Rummens, Can. J. Chem. **55**, 3007 (1977).
[39] J. H. Wilkinson and C. Reinsch, *Linear Algebra* (Springer, New York, 1971).
[40] V. Mokrushin, V. Bedanov, W. Tsang, M. R. Zachariah, and V. D. Knyazev, CHEMRATE, Version 1.19, National Institute of Standards and Technology, Gaithersburg, MD, 2002.
[41] W. Tsang, V. Bedanov, and M. R. Zachariah, J. Phys. Chem. **100**, 4011 (1996).
[42] V. D. Knyazev and W. Tsang, J. Phys. Chem. A **104**, 10747 (2000).
[43] V. D. Knyazev and W. Tsang, J. Phys. Chem. A **103**, 3944 (1999).
[44] I. V. Tokmakov and M. C. Lin, J. Am. Chem. Soc. **125**, 11397 (2003).
[45] I. V. Tokmakov and M. C. Lin, J. Phys. Chem. A **108**, 9697 (2004).
[46] R. N. Rudolph and E. C. Y. Inn, J. Geophys. Res. C: Oceans Atoms. **86**, 9891 (1981).
[47] FACSIMILE is a computer software for modeling process and chemical-reaction kinetics released by AEA Technology, Oxfordshire, United Kingdom.
[48] J. A. Kerr and M. J. Parsonage, *Evaluated Kinetic Data on Gas Phase Addition Reactions* (Butterworths, London, 1972).
[49] D. D. Davis, R. B. Klemm, W. Braun, and M. Pilling, Int. J. Chem. Kinet. **4**, 383 (1972).
[50] A. G. Baboul, L. A. Curtiss, P. C. Redfern, and K. Raghavachari, J. Chem. Phys. **110**, 7650 (1999).